Supporting Information

Imaging of Ovarian Cancers Using Enzyme Activatable Probes with Second Near-Infrared Window Emission

Ji-An Chen[a], Hongming Pan[b], Zhijun Wang[b], Jie Gao[a], Jiahui Tan[a], Zhirong Ouyang[a]

*Wei Guo[b], Xianfeng Gu[a]**

[a]Department of Medicinal Chemistry, School of Pharmacy, Fudan University, Shanghai 201301, China

[b]Department of Pharmacology, School of Pharmacy, Fudan University, Shanghai 201301, China

*Correspondence: xfgu@fudan.edu.cn

Experimental Section

1 Materials and reagents

All chemicals were purchased from commercial suppliers unless otherwise specified. ^{1}H NMR and ^{13}C spectra were recorded on a Bruker AV-400 and AV 600 MHz instruments with chemical shifts reported in ppm. Deuterated chloroform and Deuterated DMSO were used as the solvent, TMS as the internal standard. Mass spectra were measured on an HP 1100 LC-MS spectrometer. Fluorescence spectra were measured with F-7000 Fluorescence Spectrophotometer (Hitachi, Japan). NIR II fluorescence spectra were measured with QM-40 Steady State and Transient State Fluorescence Spectrometer (PTI, U.S.A.).

2 Synthesis

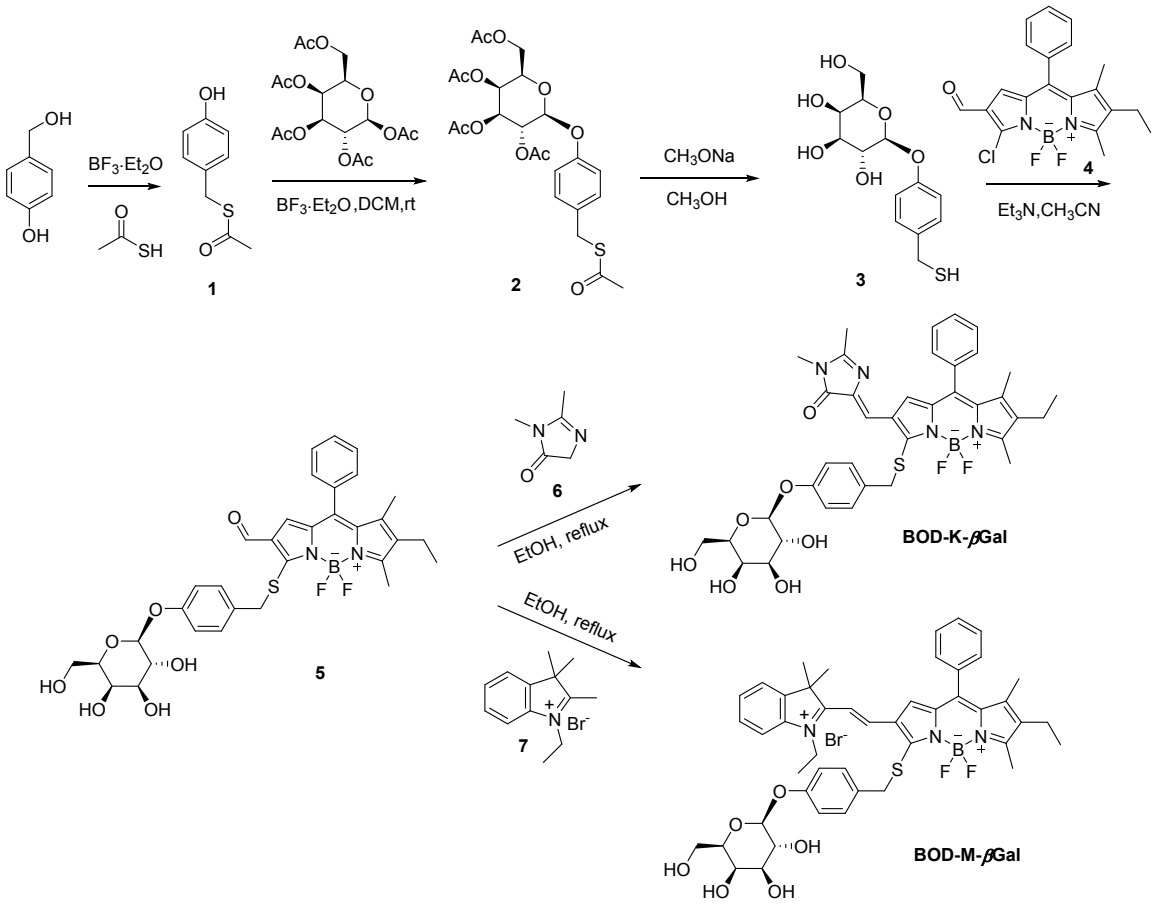

2.1 Synthesis of compound 1

To (4-hydrooxyphenyl)methanol (15 g, 120 mmol) suspended in thioacetic acid (80 mL) was added $BF_3{\cdot}OEt_2$ (2.25 mL, 16.5 mmol). After stirring for 3 h at room temperature, the solution was diluted with EtOAc (100 mL), washed with saturated $NaHCO_3$ and brine, dried over Na_2SO_4, filtered and evaporated. The crude product was purified by silica gel column (hexane: ethyl actate = 20: 1) to give **1** (16 g, 73%). ^{1}H NMR (400MHz, $CDCl_3$), δ 2.27 (s, 3H), 3.99 (s, 2H), 5.66 (s, 1H), 6.98 (d, *J* = 8.1 Hz, 2H), 7.07 (d, *J* = 8.1 Hz, 2H). ESI-MS calculated for $C_9H_{10}NaO_2S^+$ $[M+Na]^+$: 205.0, found: 205.1.

2.2 Synthesis of compound 2

To 300 mL freshly distilled DCM was added *β-D*-galactose peracetate (15.6 g, 40 mmol), **1** (14.6 g, 80 mmol) and $BF_3{\cdot}OEt_2$ (25 mL, 160 mmol). After stirring for 36 h at room temperature, the solution was diluted with DCM, washed with saturated $NaHCO_3$ and brine, dried over Na_2SO_4 and evaporated. The residue was purified by silica gel column (hexane: ethyl actate = 4: 1) to afford **2** (8.8 g, 43%). ^{1}H NMR (600 MHz, DMSO-d_6) δ 7.25 (d, *J* = 8.6 Hz, 2H), 6.92 (d, *J* = 8.6 Hz, 2H), 5.42 (d, *J* = 7.9 Hz, 1H), 5.33 (d, *J* = 3.5 Hz, 1H), 5.27 (dd, *J* = 10.4, 3.5 Hz, 1H), 5.19 (dd, *J* = 10.3, 7.9 Hz, 1H), 4.41 (t, *J* = 6.4 Hz, 1H), 4.09 (dd, *J* = 6.4, 3.8 Hz, 2H), 4.07 (s, 2H), 2.34 (s, 3H), 2.14 (s, 3H), 2.03 (s, 3H), 2.00 (s, 3H), 1.94 (s, 3H). ^{13}C NMR (151 MHz, DMSO-d_6) δ 194.83, 169.97, 169.83, 169.55, 169.21, 155.55, 132.29, 130.01, 116.47, 97.78, 70.30, 70.13, 68.33, 67.20, 61.28, 39.52, 31.83, 30.27, 20.47, 20.43, 20.39, 20.34.ESI-MS calculated for $C_{23}H_{28}NaO_{11}S^+$ $[M+Na]^+$: 535.1, found: 535.2.

2.3 Synthesis of compound 3

To 40 mL dry MeOH was added **2** (2.56 g, 5 mmol) and sodium methoxide (54 mg, 1 mmol) and stirred at room temperature for 30 min. After completion of the reaction, the mixture was neutralized with Dowex 50WX2 ion-exchange resin, filtered and evaporated to afford **3** (1.05 g, 69.4%) ready for next step. ESI-MS calculated for $C_{13}H_{18}NaO_6S^+$ $[M+Na]^+$: 325.1, found: 325.1.

2.4 Synthesis of compound 5

To 60 mL dry MeCN was added **3** (950 mg, 3.12 mmol), **4** (400 mg, 1.04 mmol) and Et_3N (14.5 μl, 0.104 mmol) under argon protection. The mixture was stirred at room temperature for 48 h. Then, the solution was diluted with MeOH and purified by silica gel column (DCM: MeOH = 15: 1) to afford **5** (296 mg, 40.7%). ^{1}H NMR (400 MHz, $CDCl_3$) δ 8.94 (s, 1H), 7.39 (m, 3H), 7.20 (m, 2H), 6.83 (d, *J* = 8.1 Hz, 2H), 6.76 (d, *J* = 8.1 Hz, 2H), 6.45 (s, 1H), 4.73 (m, 1H), 4.48 (m, 1H), 4.38 (m,

1H), 4.20 (m, 1H), 4.00 (m, 2H), 3.62 (m, 2H), 3.40 (m, 1H), 2.67 (s, 3H), 2.32 (q, *J* = 7.4 Hz, 2H), 1.39 (s, 3H), 0.97 (t, *J* = 7.4 Hz, 3H). ESI-MS calculated for $C_{33}H_{36}BF_2N_2O_7S^+$ $[M+H]^+$: 653.2, found: 653.3.

2.5 Synthesis of compound BOD-K-βGal

Compound **5** (300mg, 0.46 mmol) was dissolved in freshly distilled EtOH (20 mL), followed by the addition of compound **6** (155 mg, 1.38 mmol). The solution was stirred for 6 h at 90 °C under argon. After cooling to room temperature, the solvent was removed *in vacuo* and the residue was purified by silica gel column (DCM: MeOH = 15: 1) to afford **BOD-K-*β*Gal** (130mg, 38.1%). ^{1}H NMR (400 MHz, DMSO-d_6) δ 7.61 (d, 3H), 7.49 (d, 2H), 7.12 (s, 1H), 7.07 (d, *J* = 8.3 Hz, 2H), 6.86 (d, *J* = 8.3 Hz, 2H), 6.70 (s, 1H), 5.16 (d, *J* = 5.0 Hz, 1H), 4.88 (d, *J* = 5.0 Hz, 1H), 4.66 (d, 2H), 4.51 (d, 1H), 4.17 – 4.09 (m, 3H), 3.68 (s, 1H), 3.51 (m, 4H), 3.16 (d, 2H), 3.01 (s, 3H), 2.67 (s, 3H), 2.40 (d, 2H), 2.12 (s, 3H), 1.44 (s, 3H), 1.00 (t, *J* = 7.4 Hz, 3H). ^{13}C NMR (151 MHz, DMSO-d_6) δ 169.23, 166.99, 162.18, 156.78, 143.28, 142.99, 139.95, 138.28, 137.23, 136.09, 134.62, 132.84, 129.94, 129.44, 128.92, 128.74, 124.49, 116.55, 116.17, 101.05, 79.19, 78.97, 78.75, 75.43, 73.32, 70.22, 68.05, 60.29, 54.90, 48.62, 41.25, 39.52, 26.19, 16.53, 15.40, 13.83, 13.61, 12.17. HRMS (ESI, m/z): calculated for ESI-MS calculated for $C_{38}H_{42}BF_2N_4O_7S^+$ $[M+H]^+$: 747.2757, found: 747.2837.

2.6 Synthesis of compound BOD-M-βGal

Compound **5** (300mg, 0.46 mmol) was dissolved in freshly distilled EtOH (20 mL), followed by the addition of malononitrile (368 mg, 1.38 mmol). The solution was stirred for 6 h at 90 °C under argon. After cooling to room temperature, the solvent was removed *in vacuo* and the residue was purified by silica gel column (DCM: MeOH = 15: 1) to afford **BOD-M-*β*Gal** (104 mg, 25.1%). ^{1}H NMR (400 MHz, DMSO-d_6) δ 7.88 (d, 1H), 7.80 (m, 2H), 7.65 (m, 3H), 7.57 (m, 4H), 7.25 (d, 1H),

7.13 (s, 1H), 7.01 (d, *J* = 8.0 Hz, 2H), 6.85 (d, *J* = 8.0 Hz, 2H), 5.07 (d, 1H), 4.87 (s, 1H), 4.68 (d, 1H), 4.58 (s, 1H), 4.47 (s, 3H), 4.25 (s, 2H), 3.63 (s, 1H), 3.16 (s, 2H), 2.74 (s, 3H), 2.44 (q, 2H), 1.52 (s, 3H), 1.49 (s, 3H), 1.43 (s, 3H), 1.31 (q, 3H), 1.02 (q, 3H). ^{13}C NMR (151 MHz, DMSO-d_6) δ 180.85, 169.86, 156.80, 145.99, 144.93, 144.04, 143.17, 140.33, 139.78, 139.55, 137.43, 135.97, 132.31, 131.17, 130.58, 130.12, 129.76, 129.04, 129.00, 128.91, 128.83, 122.94, 120.62, 116.18, 114.64, 109.96, 100.61, 75.30, 73.22, 70.11, 67.87, 67.23, 67.15, 60.12, 51.64, 48.57, 41.67, 41.10, 40.06, 39.52, 26.20, 26.15, 19.96, 16.52, 13.89, 13.63, 13.52, 12.14. HRMS (ESI, m/z): ESI-MS calculated for $C_{46}H_{51}BF_2N_3O_6S^+$ $[M]^+$: 822.3560, found: 822.3573.

3 *In vitro* enzymatic assay

the probes BOD-K-*β*Gal and BOD-M-*β*Gal was used at a final concentration of 10 μM. Absorption and fluorescence spectra of the probes with *β*-Gal enzymatic reactions were performed in a 3 mL total volume of aqueous solution (phosphate-buffered saline (PBS): dimethyl sulfoxide (DMSO) = 7:3 v:v, pH = 7.4, 37 °C) in a 1 cm cuvette.

4 Cells culture and imaging

Human ovarian cancer SKOV3 cells were grown at 37 ^{o}C under a humidified 5% CO_2 atmosphere in RPMI-1640 medium (HyClone), which were supplemented with 10% fetal bovine serum (FBS, Gibco), 1% penicillin-streptomycin (Gibco). HUVECs (human umbilical vein endothelial cells were grown at 37 ^{o}C under a humidified 5% CO_2 atmosphere in Dulbecco's Eagle Medium (DMEM) supplemented with 10% fetal bovine serum (FBS, Gibco), 1% penicillin-streptomycin (Gibco). The cell counting kit-8 assay was performed to demonstrate the low cytotoxicity of the probes BOD-K-*β*Gal and BOD-M-*β*Gal.

For real-time tracking of *β*-Gal activities, SKOV3 and HUVECs cells were seeded into a glass-bottomed dish for 12 h and then cultured with BOD-K-*β*Gal (30 μM) for 8 h. Live cell images were acquired using Carl Zeiss LSM710 with a 48× objective. Green channel at 550-600 nm with λ_{ex} = 488 nm, red channel at 671-758 nm with λ_{ex} = 633 nm, ratio image generated form red to green

channel.

5 *In vivo* imaging

The animal experiments were performed in compliance with the relevant laws and institutional guidelines for the Care and Use of Research Animals established by Fudan University, and the experimental procedures were approved by our institutional review board.

To establish tumor models in 6-week-old female BALB/c nude mice, SKOV3 cells (1×10^7) suspended in 200 μl PBS were injected subcutaneously into the indicated location in nude mice. When the tumor was about 70 mm^3 (about 3 weeks after implantation, *in vivo* fluorescence imaging was carried out for targeted cancer visualization.

Two groups of mice were randomly divided, 1) probe (30 nmol) in DMSO were injected to the tumor regions and normal sites via intratumoral injection; 2) tumor-bearing mice were treated with *D*-galactose (a competitive β-gal inhibitor) for 2 h, followed by treatment with probes. Images were acquired at various time after treatment. NIR-I images were recorded using the IVIS spectrum imaging system, 633 nm was used as the excitation wavelength and the fluorescence signals were collected between 700 nm-720 nm. NIR-II images were collected via series II 900/1700 imaging system. The excitation wavelength was 808 nm and the NIR-II emission was collected form 900-1300 nm.

6 Selectivity of BOD-K-*β*Gal and BOD-M-*β*Gal

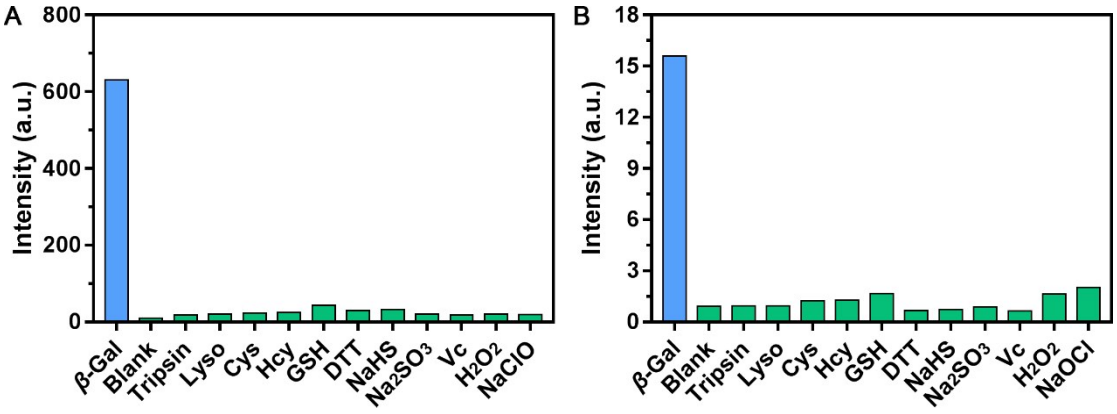

Figure S1 (A) Fluorescence responses of **BOD-K-*β*Gal** (10 μM) to various analytes (*β*-Gal (8 U), trypsin (1 kU), lysozyme (1 kU), Cys (1 mM), Hcy (1 mM), GSH (1 mM), DTT (1 mM), NaHS (1 mM), $Na_2S_2O_3$ (1 mM), Vc (1 mM), H_2O_2 (1 mM), and NaClO (1 mM)) in an aqueous system (PBS/DMSO = 7:3 v:v; pH = 7.4, 37 °C) were measured with F-7000 Fluorescence Spectrophotometer (Hitachi, Japan, λ_{em} = 715 nm, λ_{ex} = 633 nm). (B) Fluorescence responses of **BOD-M-*β*Gal** (10 μM) to various analytes (*β*-Gal (8 U), trypsin (1 kU), lysozyme (1 kU), Cys (1 mM), Hcy (1 mM), GSH (1 mM), DTT (1 mM), NaHS (1 mM), $Na_2S_2O_3$ (1 mM), Vc (1 mM), H_2O_2 (1 mM), and NaClO (1 mM)) in an aqueous system (PBS/DMSO = 7:3 v:v; pH = 7.4, 37 °C) were measured with QM-40 Steady State and Transient State Fluorescence Spectrometer (PTI, U.S.A. λem = 853 nm, λ_{ex} = 723 nm).

7 Enzyme kinetics parameters of probes against *β*-Gal

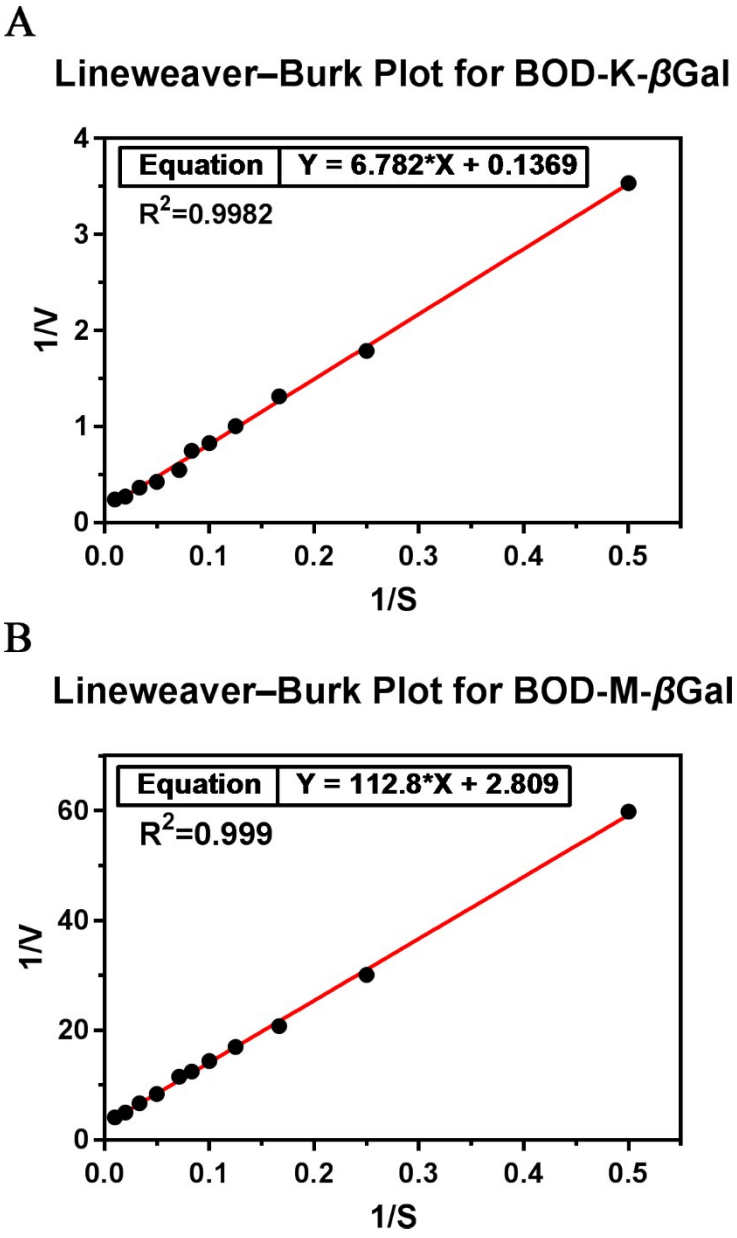

Figure S2 Plots of 1/V as function of 1/S for determining V_{max} and K_m. Utilizing Michaelis-Menten equation (1), we can get equation (2), wherein V represents the velocity and [S] represents the probe concentration, while K_m is the Michaelis constant. The slope and the intercept can be afforded by the Lineweaver–Burk Plot. Accordingly, V_{max} and K_m were determined to be 7.30 $\mu M \cdot S^{-1}$ and 49.54 μM for BOD-K-*β*Gal, and V_{max} and K_m were determined to be 0.36 $\mu M \cdot S^{-1}$ and 40.16 μM for BOD-M-*β*Gal.

$$V = V_{max} \times [S]/(K_m + [S]) \quad (1)$$

$$\frac{1}{V} = \left(\frac{K_m}{V_{max}}\right) \times \frac{1}{[S]} + \frac{1}{V_{max}} \quad (2)$$

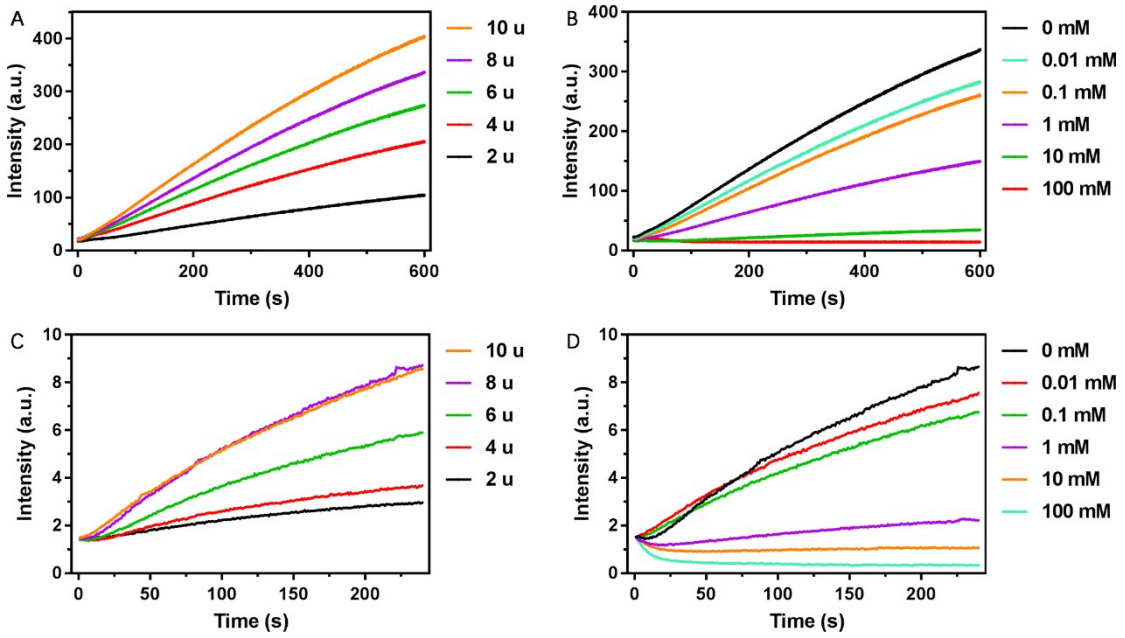

Figure S3 (A) Time dependent fluorescence intensity increment at 715 nm using 10 μM BOD-K-*β*Gal with different amounts of *β*-Gal (2, 4, 6, 8 and 10 u) in aqueous solution (PBS:DMSO = 7:3 v:v, pH = 7.4, 37 °C), λ_{ex} = 633 nm. (B) Time dependent fluorescence intensity increment at 715 nm using 10 μM BOD-K-*β*Gal and *β*-Gal (8 u) in aqueous solution (PBS:DMSO = 7:3 v:v, pH = 7.4, 37 °C) in the presence of 0, 0.01, 0.1, 1, 10, 100 mM of *D*-galactose, λ_{ex} = 633 nm. (C) Time dependent fluorescence intensity increment at 853 nm using 10 μM BOD-M-*β*Gal with different amounts of *β*-Gal (2, 4, 6, 8 and 10 u) in aqueous solution (PBS:DMSO = 7:3 v:v, pH = 7.4, 37 °C), λ_{ex} = 723 nm. (D) Time dependent fluorescence intensity increment at 853 nm using 10 μM BOD-M-*β*Gal and *β*-Gal (8 u) in aqueous solution (PBS:DMSO = 7:3 v:v, pH = 7.4, 37 °C) in the presence of 0, 0.01, 0.1, 1, 10, 100 mM of *D*-galactose, λ_{ex} = 723 nm.

8 ESI-MS spectra characterization of BOD-K-*β*Gal and BOD-M-*β*Gal reaction with *β*-gal

A

Elemental Composition Report Page 1

Single Mass Analysis
Tolerance = 5.0 PPM / DBE: min = -1.5, max = 50.0
Element prediction: Off
Number of isotope peaks used for i-FIT = 2

Monoisotopic Mass, Even Electron Ions
329 formula(e) evaluated with 1 results within limits (up to 50 best isotopic matches for each mass)
Elements Used:
C: 0-25 H: 0-26 B: 0-1 N: 0-4 O: 0-1 S: 0-4 F: 0-2

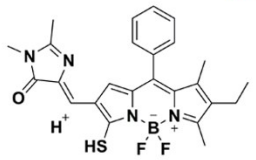

Chemical Formula: $C_{25}H_{26}BF_2N_4OS^+$
Exact Mass: 479.1883
BOD-K-SH

CC-ZHAO
ZC-WRC-03 71 (0.804) Cm (67:73)

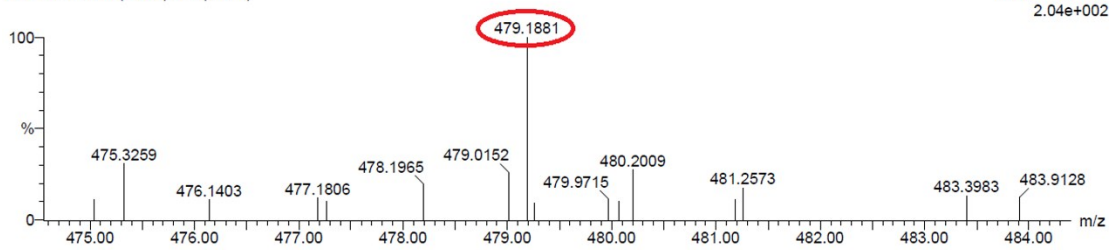

Minimum:				-1.5			
Maximum:		5.0	5.0	50.0			
Mass	Calc. Mass	mDa	PPM	DBE	i-FIT	i-FIT (Norm)	Formula
479.1881	479.1888	-0.7	-1.5	14.5	35.4	0.0	C25 H26 B N4 O S F2

B

Elemental Composition Report Page 1

Single Mass Analysis
Tolerance = 5.0 PPM / DBE: min = -1.5, max = 50.0
Element prediction: Off
Number of isotope peaks used for i-FIT = 2

Monoisotopic Mass, Even Electron Ions
203 formula(e) evaluated with 1 results within limits (up to 50 best isotopic matches for each mass)
Elements Used:
C: 33-33 H: 0-50 N: 0-5 S: 0-2 B: 0-1 F: 0-6

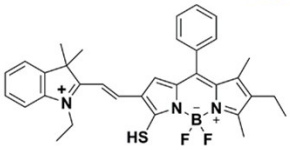

Chemical Formula: $C_{33}H_{35}BF_2N_3S^+$
Exact Mass: 554.2607
BOD-M-SH

CC-ZHAO
ZC-WRC-01 114 (1.303) Cm (114:118)

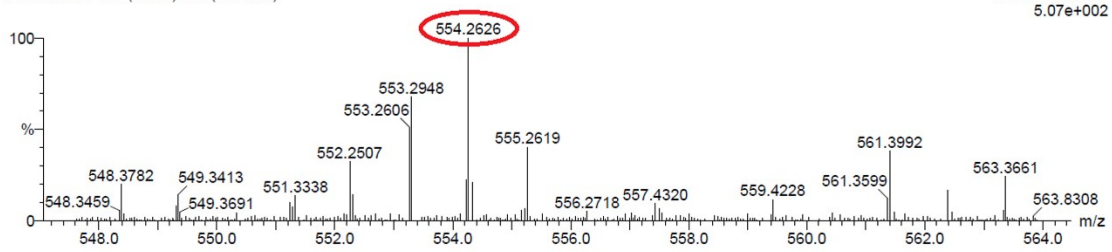

Minimum:				-1.5			
Maximum:		5.0	5.0	50.0			
Mass	Calc. Mass	mDa	PPM	DBE	i-FIT	i-FIT (Norm)	Formula
554.2626	554.2613	1.3	2.3	17.5	136.2	0.0	C33 H35 N3 S B F2

Figure S4 HRMS characterizations of the products from reactiins of (A) **BOD-K-*β*gal** + *β*-gal ($[M+H]^+$), (B) **BOD-M-*β*gal** + *β*-gal ($[M]^+$)

9 Docking results of probes against *β*-Gal

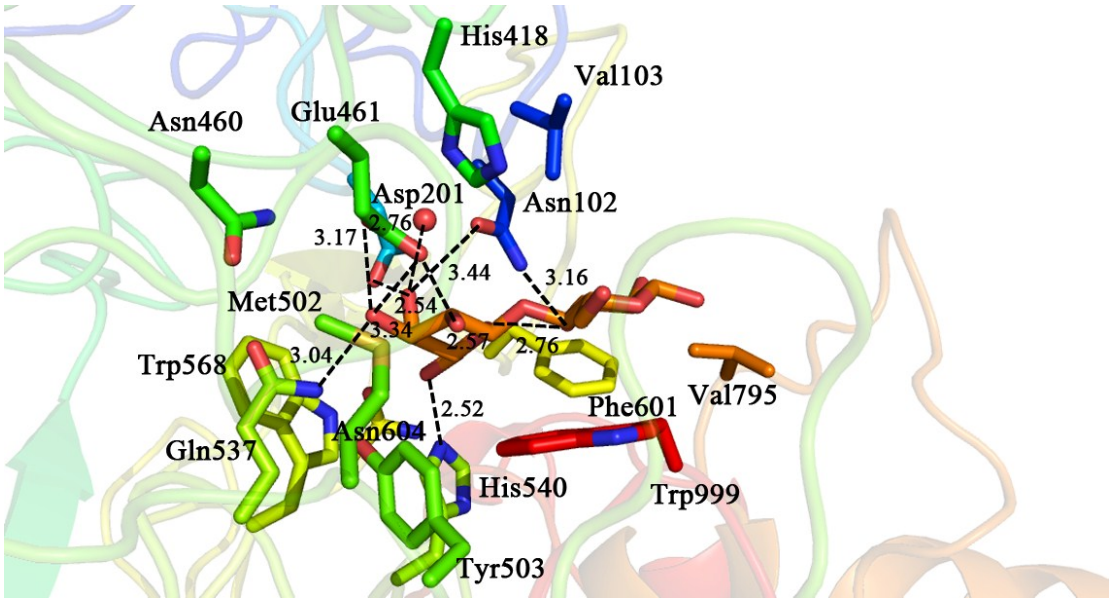

Figure S5 Binding mode of lactose (orange, sticks) with *β*-Gal (rainbow, cartoon, PDB ID 1JYN). Hydrogen bonds are illustrated as black dotted lines.

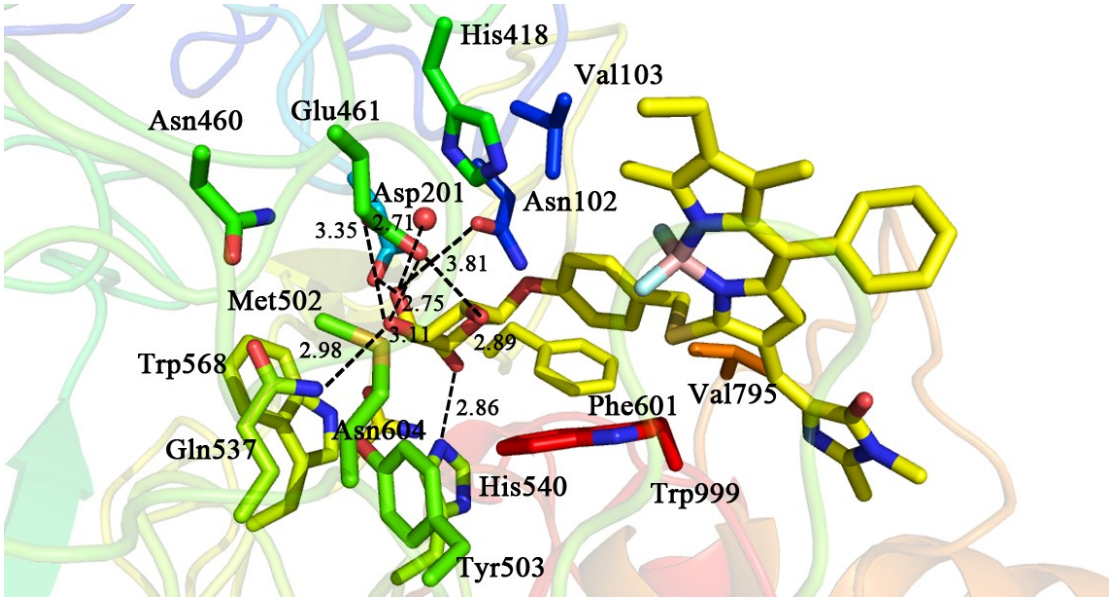

Figure S6 Docking mode of **BOD-K-*β*Gal** (yellow, sticks) with *β*-Gal (rainbow, cartoon, PDB ID 1JYN). Hydrogen bonds are illustrated as black dotted lines.

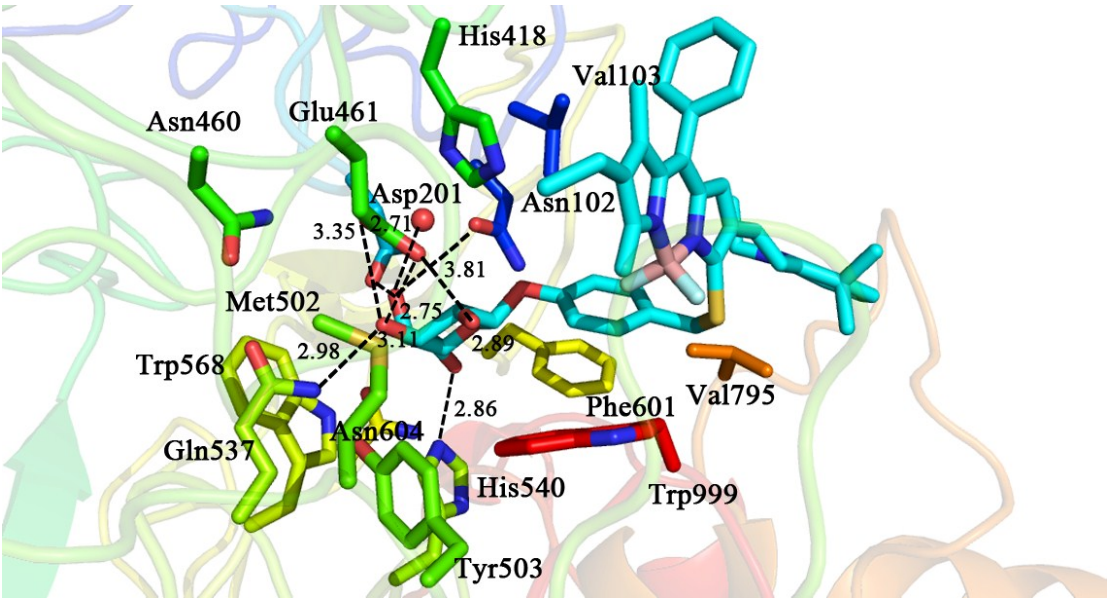

Figure S7 Docking mode of **BOD-M-*β*Gal** (blue, sticks) with *β*-Gal (rainbow, cartoon, PDB ID 1JYN). Hydrogen bonds are illustrated as black dotted lines.

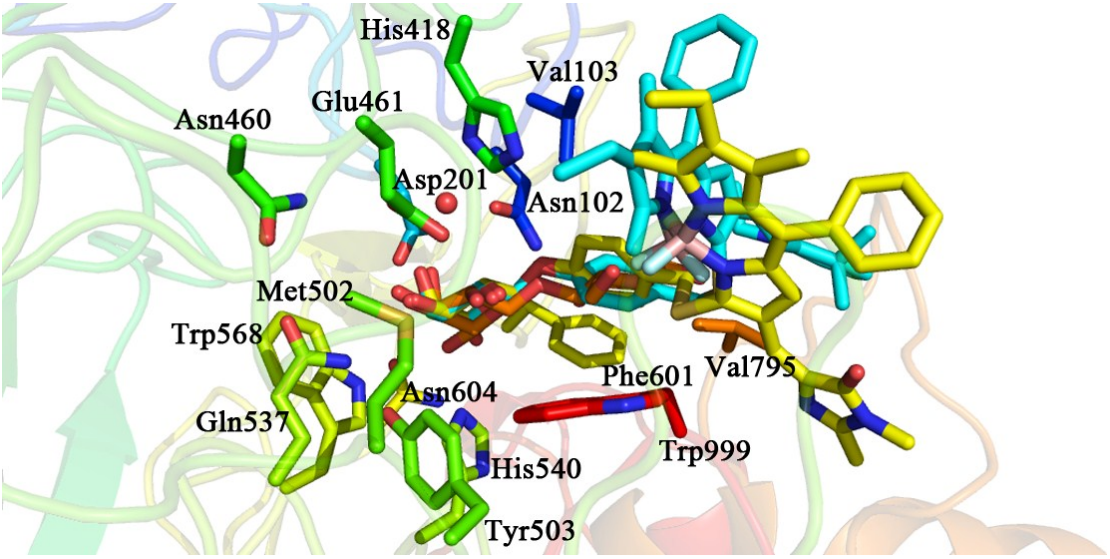

Figure S8 Aligned structures of lactose (orange, sticks), **BOD-K-*β*Gal** (yellow, sticks) and **BOD-M-*β*Gal** (blue, sticks) in *β*-Gal binding pocket (rainbow, cartoon, PDB ID 1JYN).

10 Cytotoxicity of BOD-K-*β*Gal and BOD-M-*β*Gal

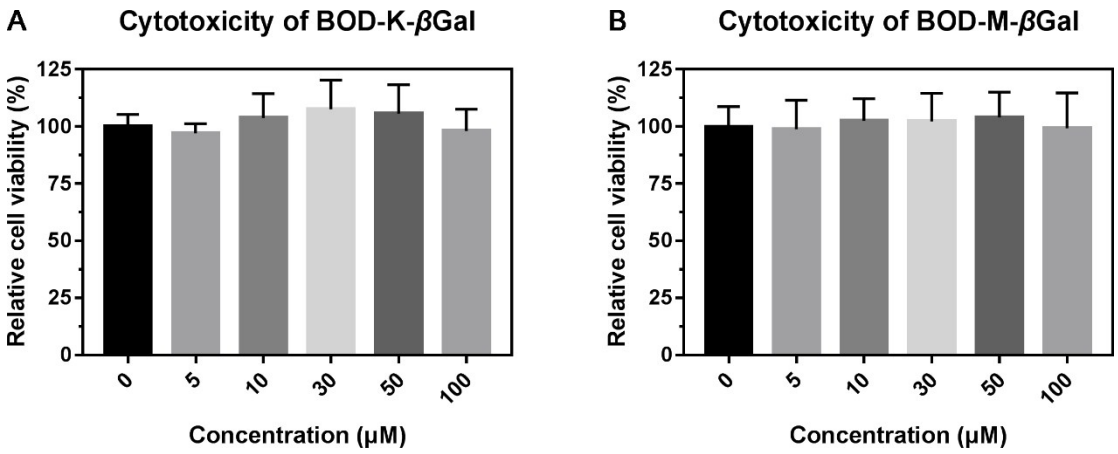

Figure S9 Relative *vitro* viability of HUVECs after incubation for 24 h with (A) **BOD-K-*β*Gal** and (B) **BOD-M-*β*Gal** at various concentrations.

11 NIR-I and NIR-II imaging capability of BOD-M-*β*Gal

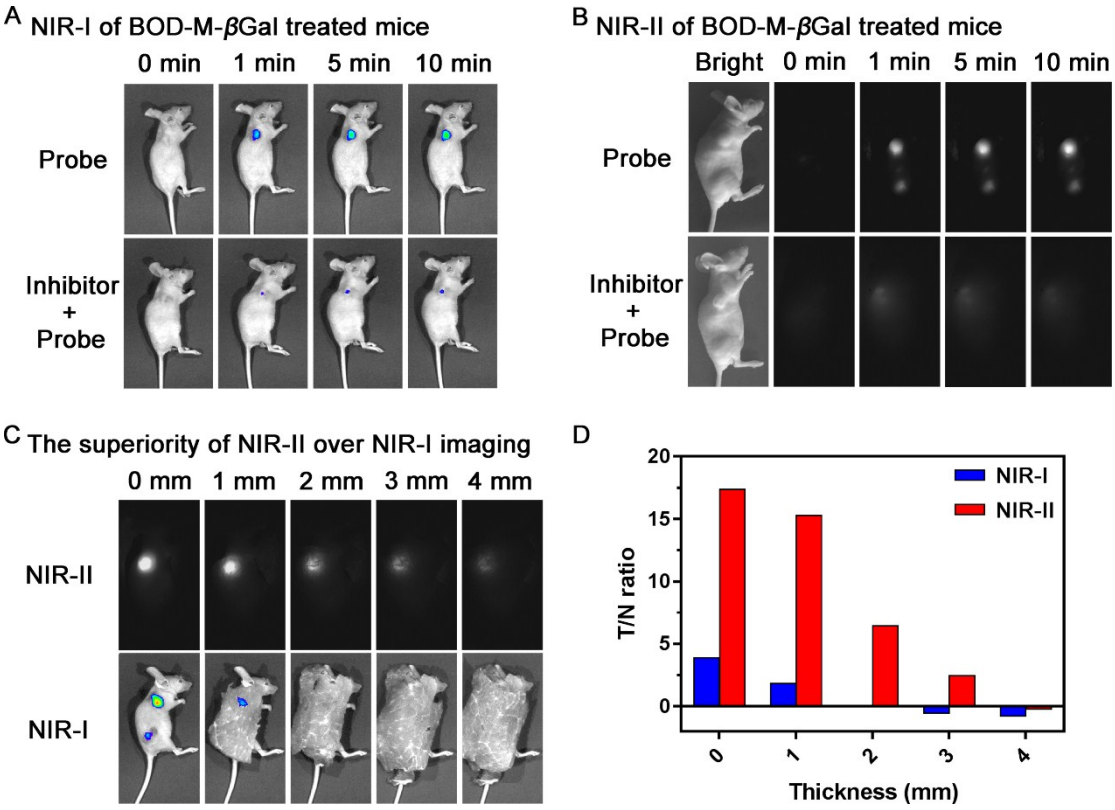

Figure S10 Ovarian tumors visualization in the SKOV3 tumor-bearing mouse model. (A) Time-dependent NIR-I imaging of mice injected with **BOD-M-*β*Gal** (30 nmol) or **BOD-M-*β*Gal** + ***D*-galactose** (0.03 mmol). (B) Time-dependent NIR-II imaging of mice injected with **BOD-M-*β*Gal** (30 nmol) or **BOD-M-*β*Gal** + ***D*-galactose** (0.03 mmol). (C) Validation of the superiority of NIR-II over NIR-I imaging using **BOD-M-*β*Gal** in a simulated deep-tissue setting at both NIR-I mode and NIR-II mode. (D) The Tumor-to-Normal Ratio (T/N) correlated with the thickness of pork tissues via NIR-I and NIR-II mode of **BOD-M-*β*Gal**. $SNR = \frac{\sum_i (x_i - \bar{x}_{BG})}{\sigma_{BG}}$. x_i is the fluorescence intensity of samples covered by the different thicknesses of pork tissues. x_{BG} is the fluorescence intensity of normal tissues. σ_{BG} is the standard deviation in the normal tissues region.

12 The Tumor-to-Normal Tissue ratio (T/N) at the different thicknesses of pork tissues with NIR-II and NIR-I mode via BOD-M-*β*Gal and BOD-K-*β*Gal

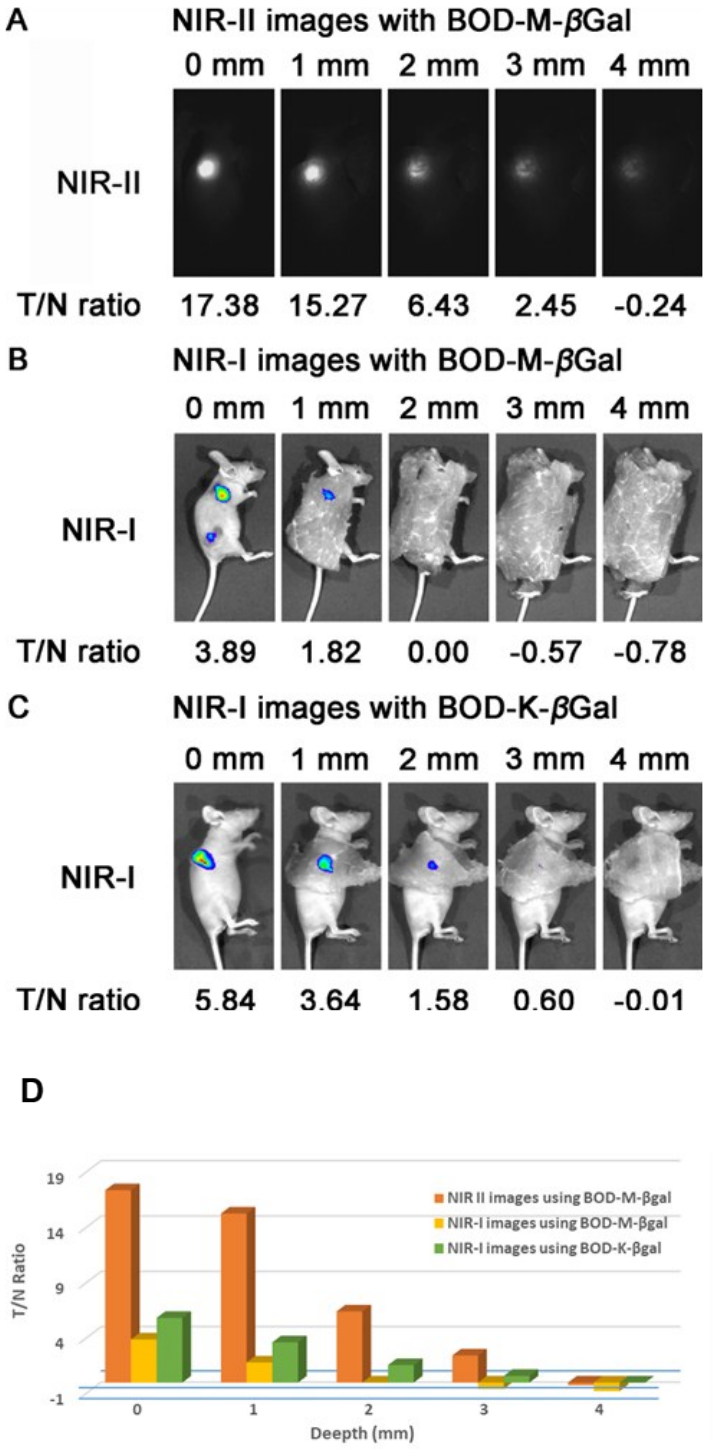

Figure S11 The Tumor-to-Normal Tissue ratio (T/N) at the different thicknesses of pork tissues with NIR-II and NIR-I mode via BOD-M-*β*Gal and BOD-K-*β*Gal.

13 Characterization of intermediate compounds, BOD-K-*β*Gal and BOD-M-*β*Gal

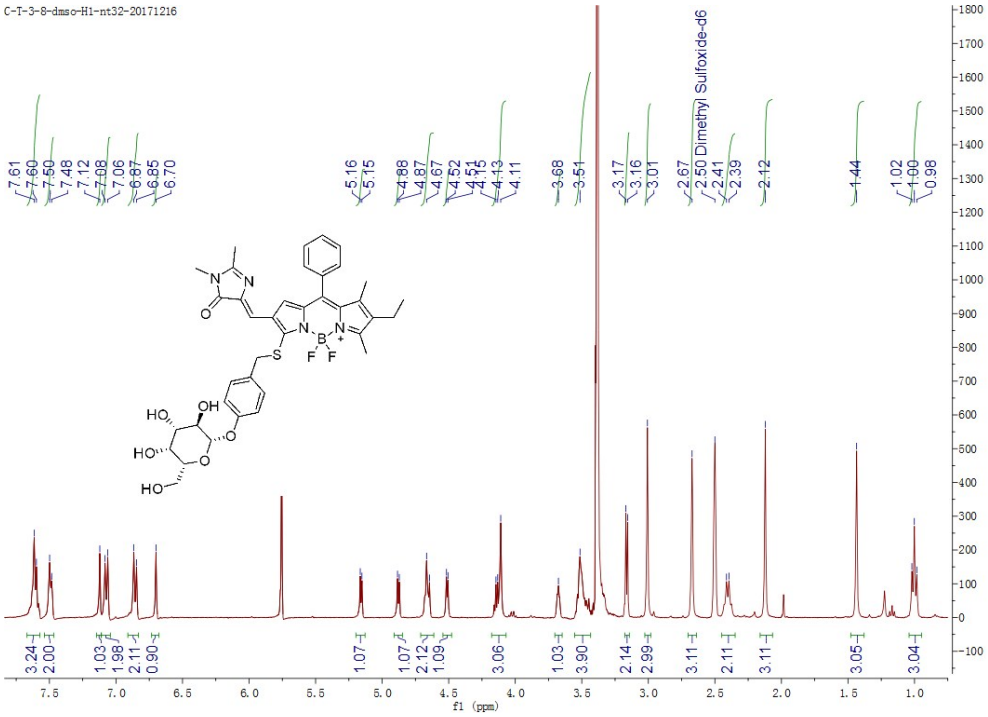

Figure S12 ^{1}H NMR spectrum of **BOD-K-*β*Gal** in DMSO-d_6

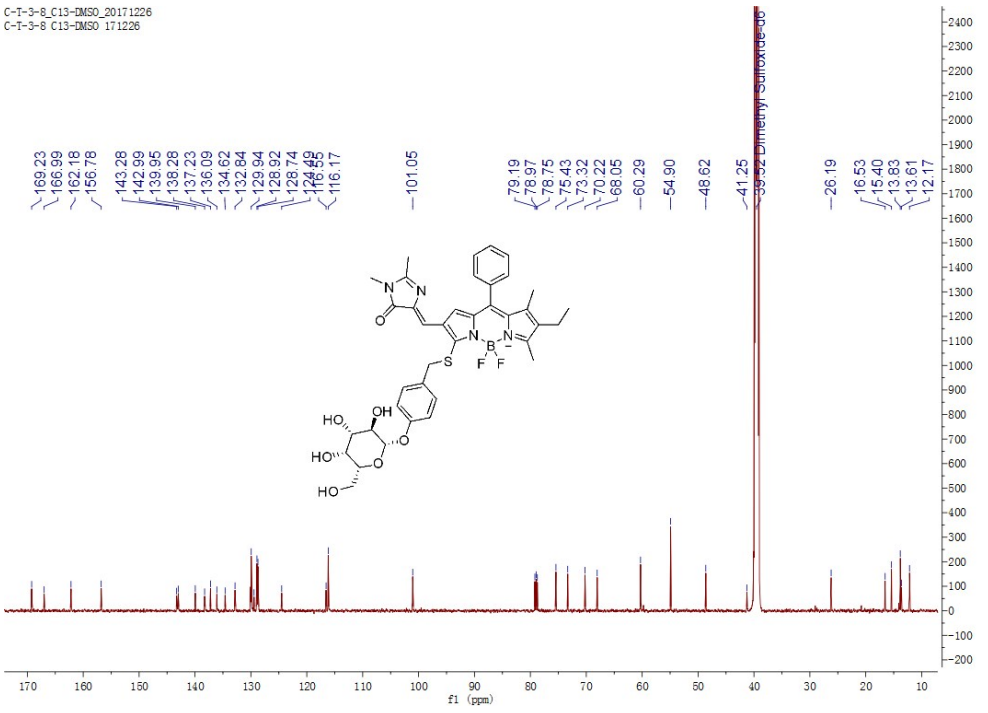

Figure S13 ^{13}C NMR spectrum of **BOD-K-*β*Gal** in DMSO-d_6

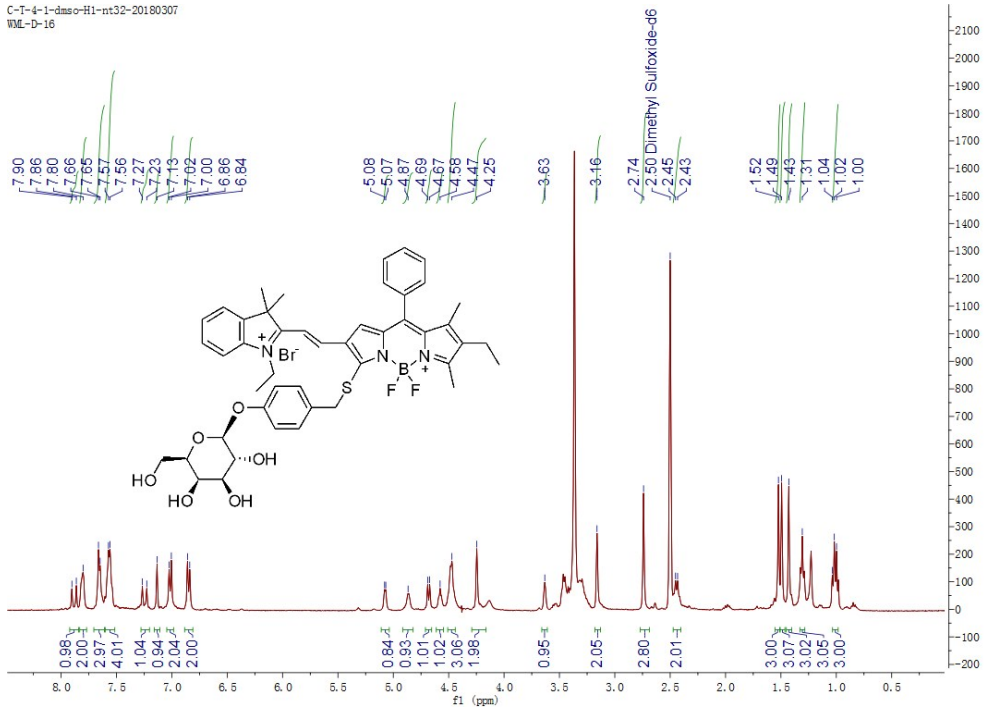

Figure S14 ^{1}H NMR spectrum of **BOD-M-*β*Gal** in DMSO-d_6

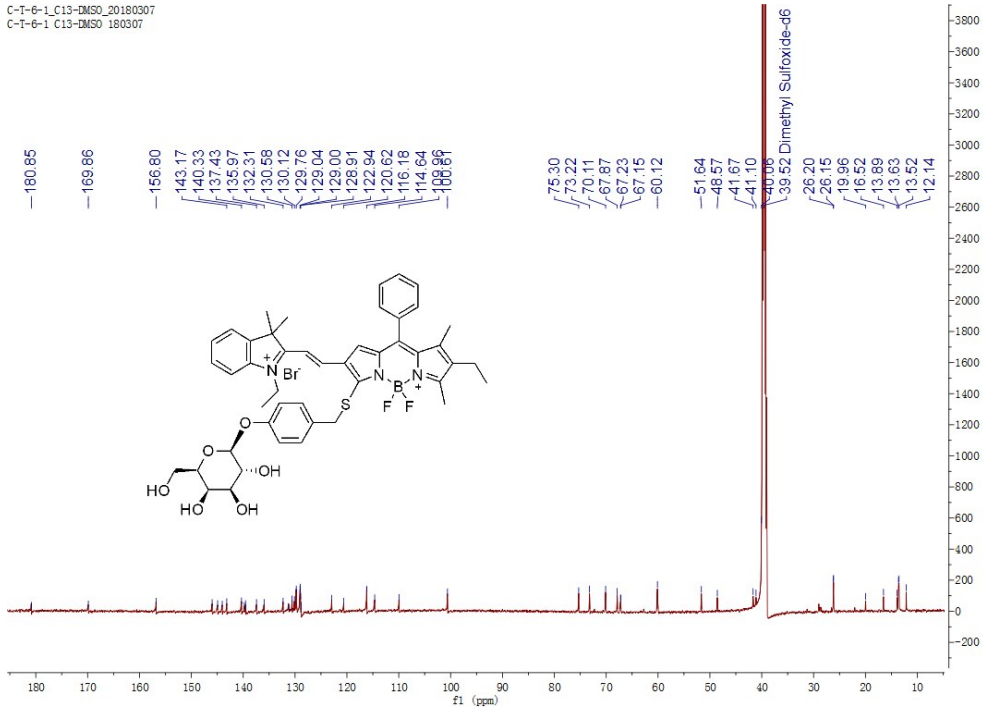

Figure S15 ^{13}C NMR spectrum of **BOD-M-*β*Gal** in DMSO-d_6

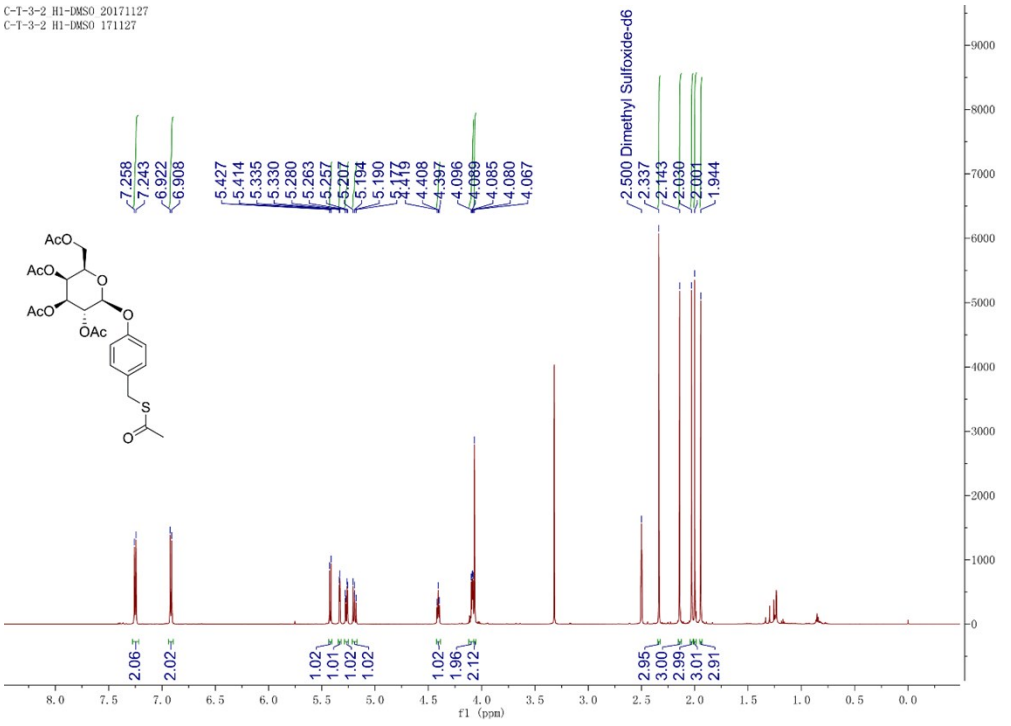

Figure S16 [1]H NMR spectrum of **2** in DMSO-d_6

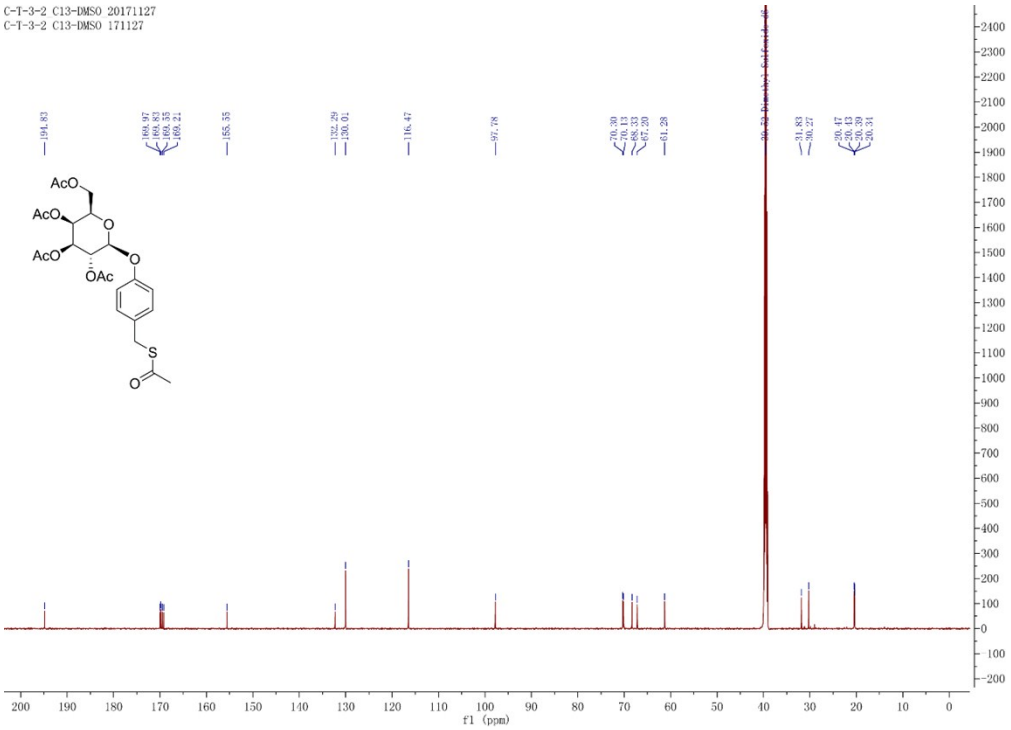

Figure S17 [13]C NMR spectrum of **2** in DMSO-d_6

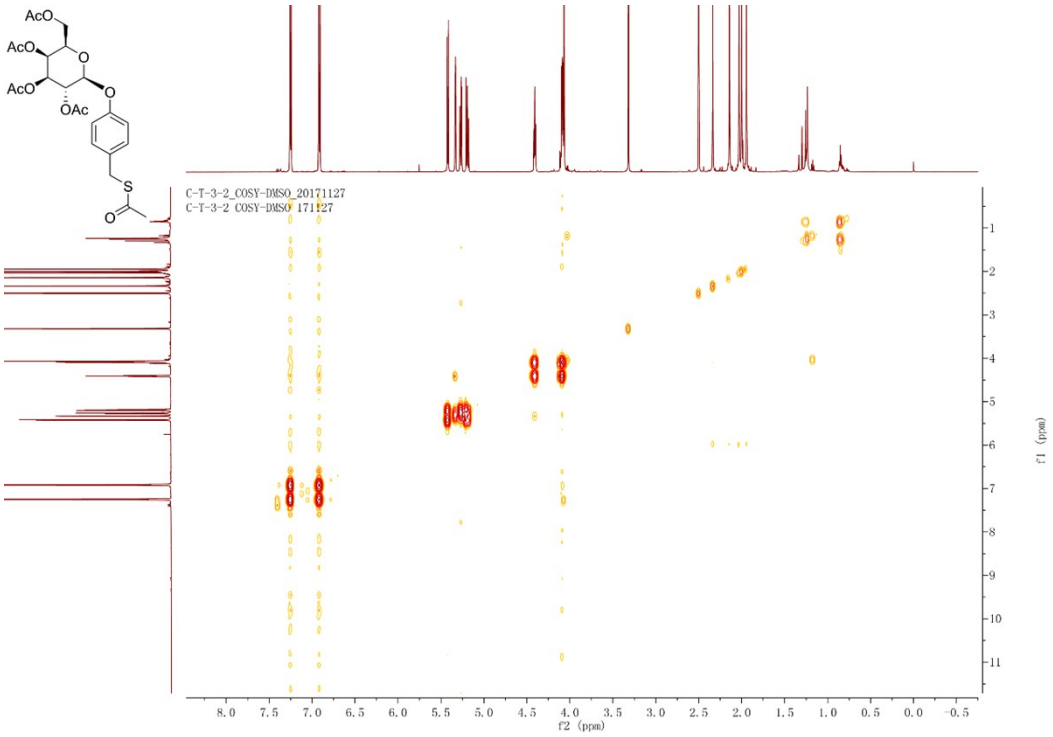

Figure S18 COSY spectrum of **2** in DMSO-d_6

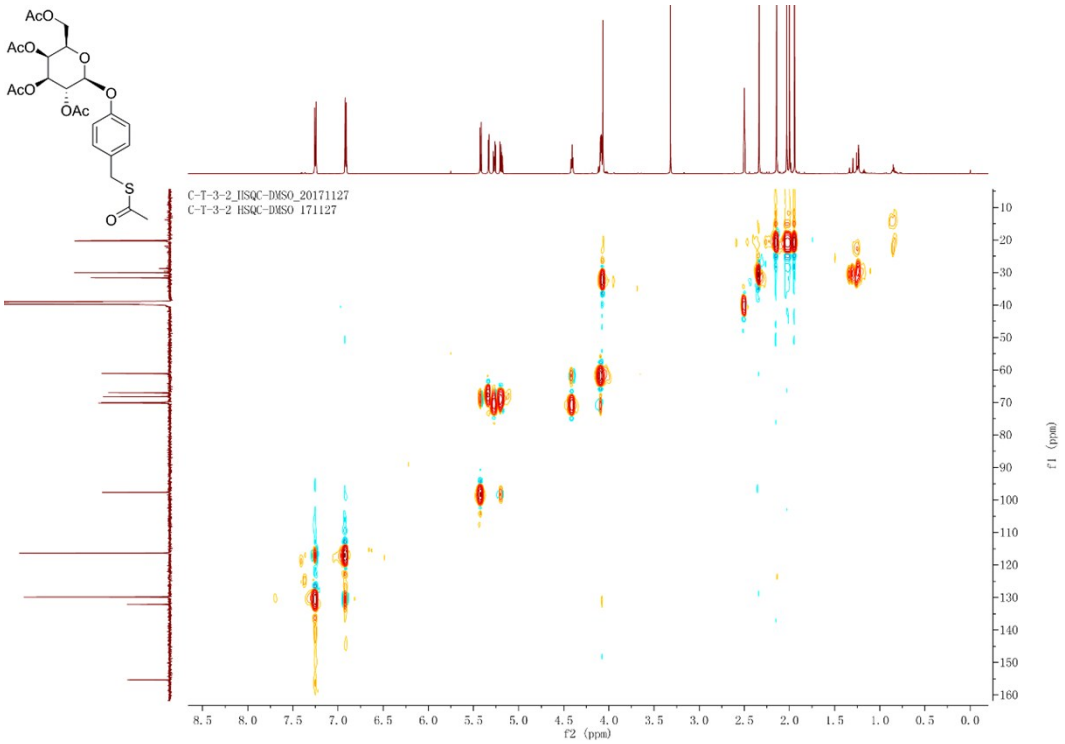

Figure S19 HSQC spectrum of **2** in DMSO-d_6

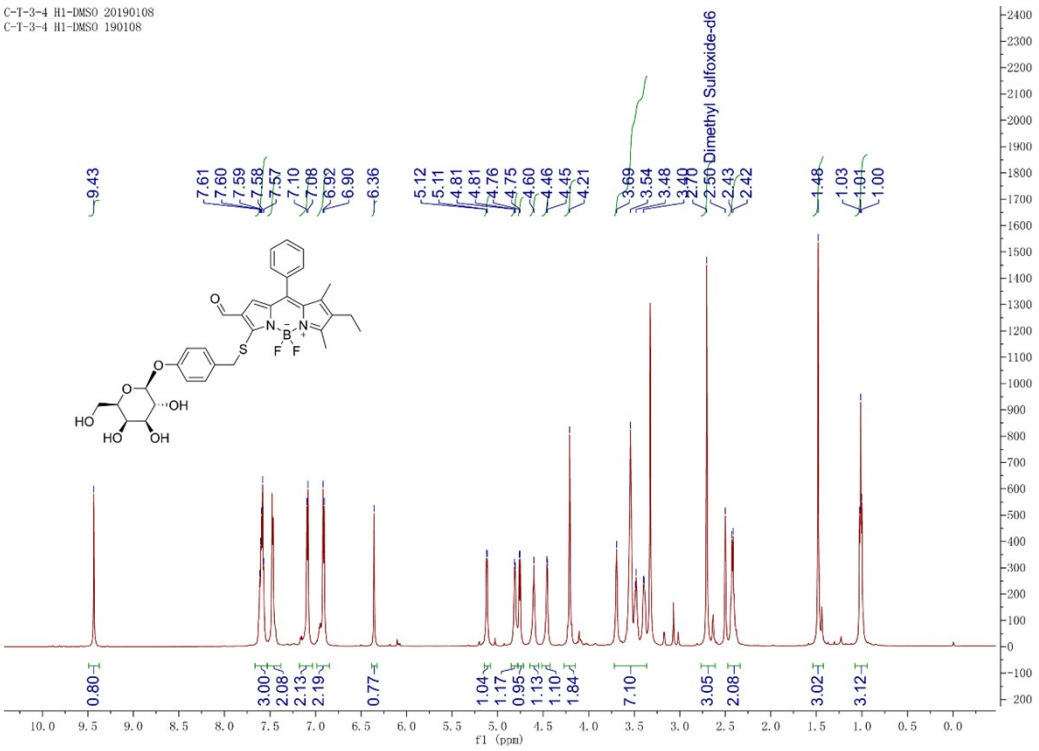

Figure S20 ^{1}H NMR spectrum of **5** in DMSO-d_6

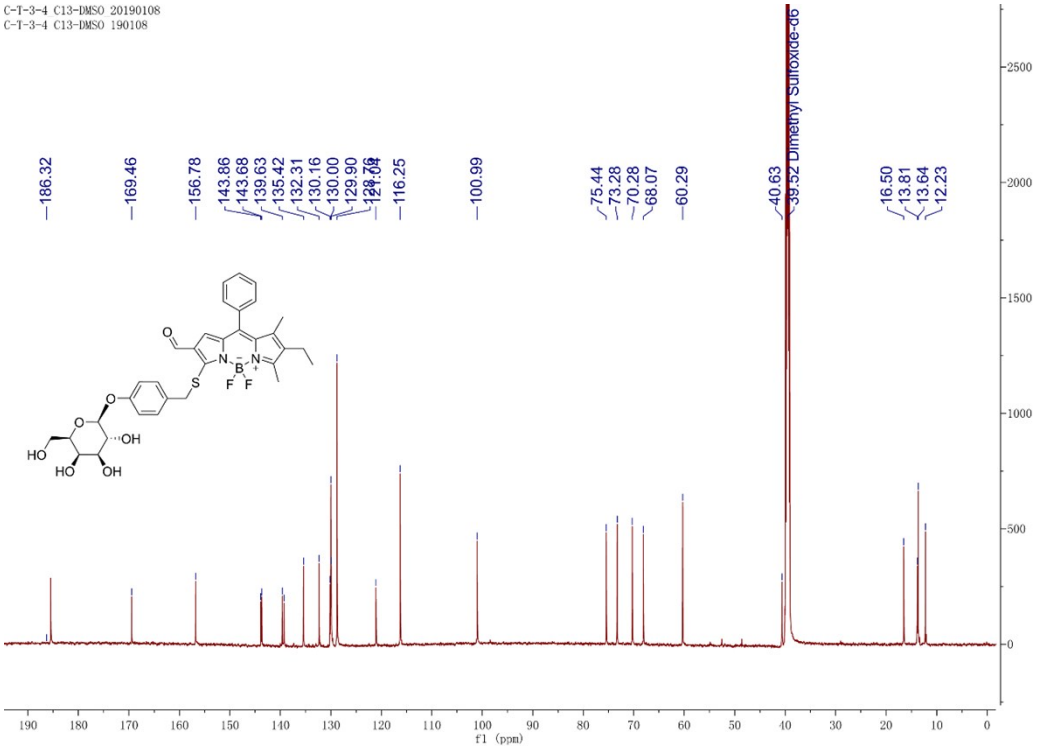

Figure S21 ^{13}C NMR spectrum of **5** in DMSO-d_6